MARTIN MARIETTA ENERGY SYSTEMS LIBRARIES
3 4456 0361510 3

CENTRAL RESEARCH LIBRARY
DOCUMENT COLLECTION

ORNL-2966
UC-34 – Physics and Mathematics

DISSOCIATION OF H_2^+ BY HYDROGEN

H. Postma
D. P. Hamblen

CENTRAL RESEARCH LIBRARY
DOCUMENT COLLECTION
LIBRARY LOAN COPY
DO NOT TRANSFER TO ANOTHER PERSON
If you wish someone else to see this document, send in name with document and the library will arrange a loan.

OAK RIDGE NATIONAL LABORATORY
operated by
UNION CARBIDE CORPORATION
for the
U.S. ATOMIC ENERGY COMMISSION

Printed in USA. Price $0.50. Available from the

Office of Technical Services
Department of Commerce
Washington 25, D.C.

LEGAL NOTICE

This report was prepared as an account of Government sponsored work. Neither the United States, nor the Commission, nor any person acting on behalf of the Commission:

A. Makes any warranty or representation, expressed or implied, with respect to the accuracy, completeness, or usefulness of the information contained in this report, or that the use of any information, apparatus, method, or process disclosed in this report may not infringe privately owned rights; or

B. Assumes any liabilities with respect to the use of, or for damages resulting from the use of any information, apparatus, method, or process disclosed in this report.

As used in the above, "person acting on behalf of the Commission" includes any employee or contractor of the Commission, or employee of such contractor, to the extent that such employee or contractor of the Commission, or employee of such contractor prepares, disseminates, or provides access to, any information pursuant to his employment or contract with the Commission, or his employment with such contractor.

ORNL-2966

Contract No. W-7405-eng-26

THERMONUCLEAR EXPERIMENTAL DIVISION

DISSOCIATION OF H_2^+ BY HYDROGEN

H. Postma
D. P. Hamblen

DATE ISSUED

NOV 28 1960

OAK RIDGE NATIONAL LABORATORY
Oak Ridge, Tennessee
operated by
UNION CARBIDE CORPORATION
for the
U. S. ATOMIC ENERGY COMMISSION

MARTIN MARIETTA ENERGY SYSTEMS LIBRARIES
3 4456 0361510 3

CONTENTS

Abstract 1

Introduction 1

Apparatus 1

Procedure 3

Calculation and Analysis 3

Results 5
- Cross Sections 5
- Angular Distributions 6

References Cited 8

DISSOCIATION OF H_2^+ BY HYDROGEN

H. Postma D. P. Hamblen

ABSTRACT

The dissociation cross section of H_2^+ by hydrogen has been measured over the energy range from 200 through 600 kev. An H_2^+ beam incident upon a differentially pumped hydrogen gas target was electrostatically analyzed for H_2^+ and the H^0 and H^+ dissociation products. The charged particles were detected by a Faraday cup and the neutral particles by a secondary-electron-emission collector. The measured total loss cross section (in cm^2 per gas atom) for H_2^+ was 7.80×10^{-17} at 200 kev, 5.81×10^{-17} at 300 kev, 4.95×10^{-17} at 400 kev, 4.52×10^{-17} at 450 kev, 4.09×10^{-17} at 500 kev, and 3.86×10^{-17} at 600 kev.

The measured proton production cross section (in cm^2 per gas atom) was 9.53×10^{-17} at 200 kev, 7.80×10^{-17} at 300 kev, 6.61×10^{-17} at 400 kev, 6.65×10^{-17} at 450 kev, 6.42×10^{-17} at 500 kev, and 6.03×10^{-17} at 600 kev. Both the total loss cross section for H_2^+ and the proton production cross section are in close agreement with the results reported by Sweetman for energies 200 through 500 kev, and with the results reported by Barnett for energies 500 through 600 kev.

INTRODUCTION

The cross section for dissociation of H_2^+ by gases has been measured over a wide energy range by several investigators. The target gas hydrogen has received the most attention. Nonetheless, the measured cross sections offer a wide variety of choices – the absolute cross sections have been in disagreement by as much as a factor of 3 in the region of present thermonuclear interest (100 through 600 kev). The present experiment resolved these discrepancies.

APPARATUS

Figure 1 displays a schematic of the apparatus. An ion beam from the high-voltage accelerator is magnetically analyzed to give H_2^+ of a known energy. The ions are incident first upon aperture A_1 ($\frac{1}{8}$ in. in diameter by $\frac{1}{4}$ in. thick), which collimates the major portion of the beam, and then upon aperture A_2 ($\frac{1}{16}$ in. in diameter by $\frac{1}{2}$ in. thick), which further defines the beam. The 15-cm (l_1) chamber enclosed by apertures A_1 and A_2 is pumped by a baffled oil-diffusion pump which maintains a large pressure difference between the gas chamber and the preceding beam tube assembly. Pressures read by ionization gages P_1 and P_g were in a ratio of 1:100 under operating conditions. The H_2^+ interacts with the hydrogen gas in the target chamber, and then H_2^+ together with the dissociated particles H^0 and H^+ exit through a motor-driven slit (0.008 in. wide by $\frac{3}{4}$ in. long) whose travel extends 1 in. in a direction perpendicular to the beam. The pressure in the gas cell is maintained at a constant value by the balance between gas flow inward through the needle valve and flow outward through aperture A_2 and slit S. This pressure is measured to within 4% accuracy by a liquid-nitrogen-trapped mercury McLeod gage. The emerging particles are energy-analyzed by a set of electrostatic deflection plates whose center is situated 20 cm (l_2) from slit S. A baffled oil-diffusion pump in chamber AC maintained a pressure-difference ratio of 1:100 as read by ionization gages P_2 and P_g. The charged particles were detected by a Faraday cup and the neutral particles by a secondary-electron-emission collector. The resulting currents were measured by an electrometer, displayed on a recorder, and integrated over the path of travel of the slit.

Both n, the density of hydrogen gas, and l, the effective length of the gas cell over which n is constant, comprise the areal density (nl) of the target. The target gas H_2 was commercial-grade spectroscopically pure and was introduced into the target chamber by an adjustable needle valve

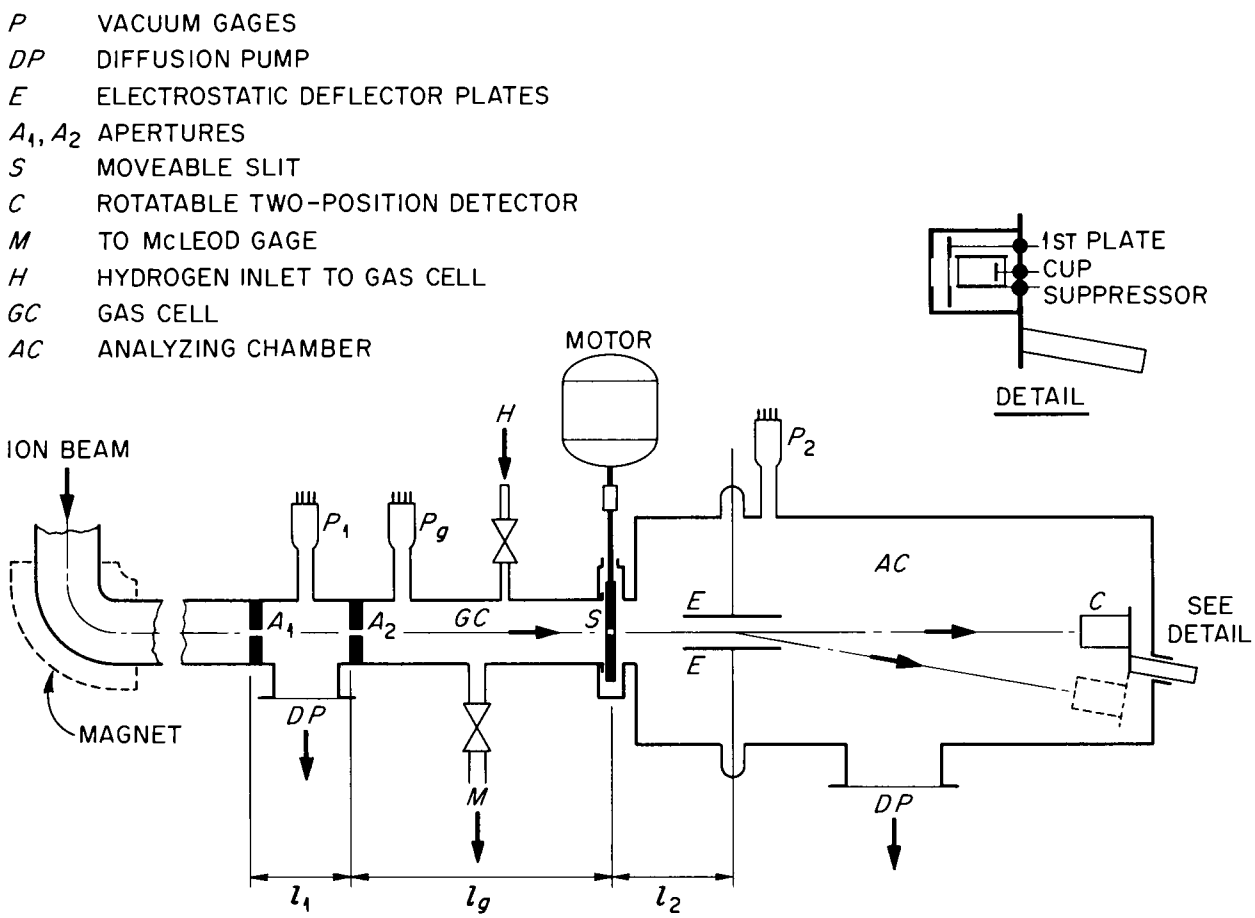

Fig. 1. Schematic of Apparatus.

after passing over a liquid-nitrogen trap. The effective length of the cell was the geometrical length l_g of the cell (44.7 cm) plus a calculated length l_s due to gas streaming from the cell in the direction of the beam through the apertures plus a length l_b due to background pressures in the immediate region of the cell. The streaming length was calculated in the manner used to determine streaming from molecular beam ovens (*1*), and it adds a length of the order of the diameter of each aperture (0.3 cm). The additional length arising from background pressures was found from the ratio of pressure in that region of interest to the pressure in the gas cell, or:

$$l_b = \frac{l_1 P_1}{P_g} + \frac{l_2 P_2}{P_g} .$$

The additional length l_b was typically 0.3 cm over the wide range of operating pressures. The effective length l used in calculation of the cross sections was the sum of these lengths:

$$l = l_g + l_s + l_b .$$

The effective length ranged from 45.1 to 45.4 cm, depending upon the operating pressure of the cell.

The details of the Faraday cup and the secondary-electron collector are shown in the insert of Fig. 1. The aperture of the detector was a 1-in. square. The first plate suppressed electrons leaving the Faraday cup assembly and was biased at −115 v. The Faraday cup assembly was a square-plate "cup" surrounded by a "square-box suppressor." When a positive beam was detected (either H^+ or H_2^+), this suppressor was biased at −22.5 v to prevent secondary electrons (emitted when the beam hit the cup) from leaving

the cup. An electrometer between the cup and ground measured the current of the impinging beam. This same assembly was also used to detect a neutral beam (either H^0 or $H_2{}^0$); in this case, the secondary electrons emitted when the neutral beam struck the cup were collected on the square-box suppressor by biasing the cup at −22.5 v. An electrometer between the suppressor and ground measured the secondary-electron emission current. This method of collecting electrons was used also to detect the electrons resulting from H^+ and $H_2{}^+$ striking the cup. The bias voltages were experimentally chosen so that the number of particles detected was independent of the voltage applied. In summary: The voltage on the electrostatic plates and the position of the detector determined whether a neutral beam or H^+ beam or $H_2{}^+$ beam entered the detector. Then, when the cup was connected to the electrometer and the suppressor biased at −22.5 v, only the charged beams were measured. However, when the suppressor was connected to the electrometer and the cup biased at −22.5 v, then secondary-electron emission current was measured.

PROCEDURE

After the energy was selected and a magnetic analysis of the beam had been made, the gas cell and the detector chamber were aligned to permit the maximum beam to pass through the target chamber. This beam current was usually 3×10^{-6} amp of $H_2{}^+$. The detector was centered with respect to the beam, and the bias was adjusted on its electrodes to obtain the saturation current for both the Faraday cup detector and the secondary-electron-emission collector. The detector was then positioned off axis, and the electrostatic deflection voltage was increased to select either the H^+ or $H_2{}^+$ to enter the detector. The target gas was introduced into the collision chamber, and its pressure measured by the McLeod gage; pressures P_1, P_2, and P_g were also noted. Because the dissociation products have acquired energy from becoming unbound, there is a spread in angle of the H^+ and H^0 about the primary $H_2{}^+$ beam. The exit slit of the gas chamber was scanned across this spread, and the resulting beam current collected by the detector was integrated to give the complete contribution of the spread; a slit was necessary to retain large pressure differences between the collision chamber and the detector chamber. The following currents were measured: $H_2{}^+$ in in the Faraday cup (FC), H^+ in the FC, $H_2{}^+ + H^+$ in the FC, H^0 in the secondary-electron collector (SEC), H^+ in the SEC, $H_2{}^+$ in the SEC, and $(H_2{}^+ + H^+ + H^0)$ in the SEC. Certain checks had to be satisfied: no data was accepted if any of the measured beam currents drifted by 7% or more during a measurement of all the above currents; the sums of the individual currents had to equal (within 2%) the measured sum of the currents [e.g., $I(H_2{}^+) + I(H^+) = I(H_2{}^+ + H^+)$ in the FC; and $I(H^0) + I(H_2{}^+) + I(H^+) = I(H^0 + H_2{}^+ + H^+)$ in the SEC]. From the integration and graphical display of these currents, it was possible to calculate the dissociation cross section and angular spread of the beam.

The pressure in the cell was then changed, and a set of currents corresponding to this new pressure was measured at the same energy. Such sets of currents for several different gas pressures as well as background pressure were made. The cross sections could be found from the functional change of current ratios with nl; this is seen in the next section.

The measured neutral current $I(H^0)$ was corrected to an equivalent Faraday cup current by dividing the measured SEC current by the product of ratios of $I(H^+)$SEC/$I(H^+)$FC and $I(H^0)$SEC/$I(H^+)$SEC. The first ratio came from the measurements of these currents during a run, and the second ratio came from the measurements of Barnett and Reynolds (*2*). This "Faraday cup equivalent" neutral current was used throughout subsequent calculations.

In several runs, the magnetic shielding around the gas cell was varied, and magnetic fields were introduced to demonstrate that this shielding was adequate to prevent stray magnetic fields from affecting the cross section.

CALCULATION AND ANALYSIS

In the energy range of our interest, the loss of $H_2{}^+$ occurs in the following modes:

Mode	Cross Section
$H_2{}^+ \longrightarrow H^0 + H^+$	σ_1
$H_2{}^+ \longrightarrow 2H^+$	σ_2
$H_2{}^+ \longrightarrow 2H^0$	σ_3
$H_2{}^+ \longrightarrow H_2{}^0$	σ_4

If one assumes that only cross sections σ_1 and σ_2 are important [Sweetman's experimental results (3) show the relative importance of these cross sections], then the cross sections are related to measured currents in the following manner:

$$\frac{I(H_2^+)}{I_0} = e^{-(\sigma_T nl + A)} , \qquad (1)$$

$$\frac{I(H^0)}{I_0} = \frac{\sigma_1 nl + B}{\sigma_T nl + A} [1 - e^{-(\sigma_T nl + A)}] , \qquad (2)$$

$$\frac{I(H^+) - I(H^0)}{2I_0} = \frac{\sigma_2 nl + C}{\sigma_T nl + A} [1 - e^{-(\sigma_T nl + A)}] , \qquad (3)$$

where

$$I_0 = I(H_2^+) + \frac{I(H^0) + I(H^+)}{2} ,$$

$\sigma_T = \sigma_1 + \sigma_2$ = total loss cross section.

Another combination of these cross sections is convenient to use: $\sigma_p = \sigma_1 + 2\sigma_2$, the proton production cross section.

In the above expressions, nl is the areal density found by the methods outlined in the Apparatus section of this report. The letters A, B, and C are the lumped effects which arise from background dissociation by slits and residual gas in the system. The effects of these backgrounds are eliminated by plotting the following expressions [derived from Eqs. (1), (2), and (3)] vs nl. The slope of the resulting lines gives σ_T, σ_1, and σ_2, and the intercepts give A, B, and C (see Fig. 2):

$$\sigma_T nl + A = -\log_e \frac{I(H_2^+)}{I_0} , \qquad (1')$$

$$\sigma_1 nl + B = \frac{I(H^0)}{I_0} \left\{ - \frac{\log_e [I(H_2^+)/I_0]}{1 - [I(H_2^+)/I_0]} \right\} = \frac{I(H^0)}{I_0} K , \qquad (2')$$

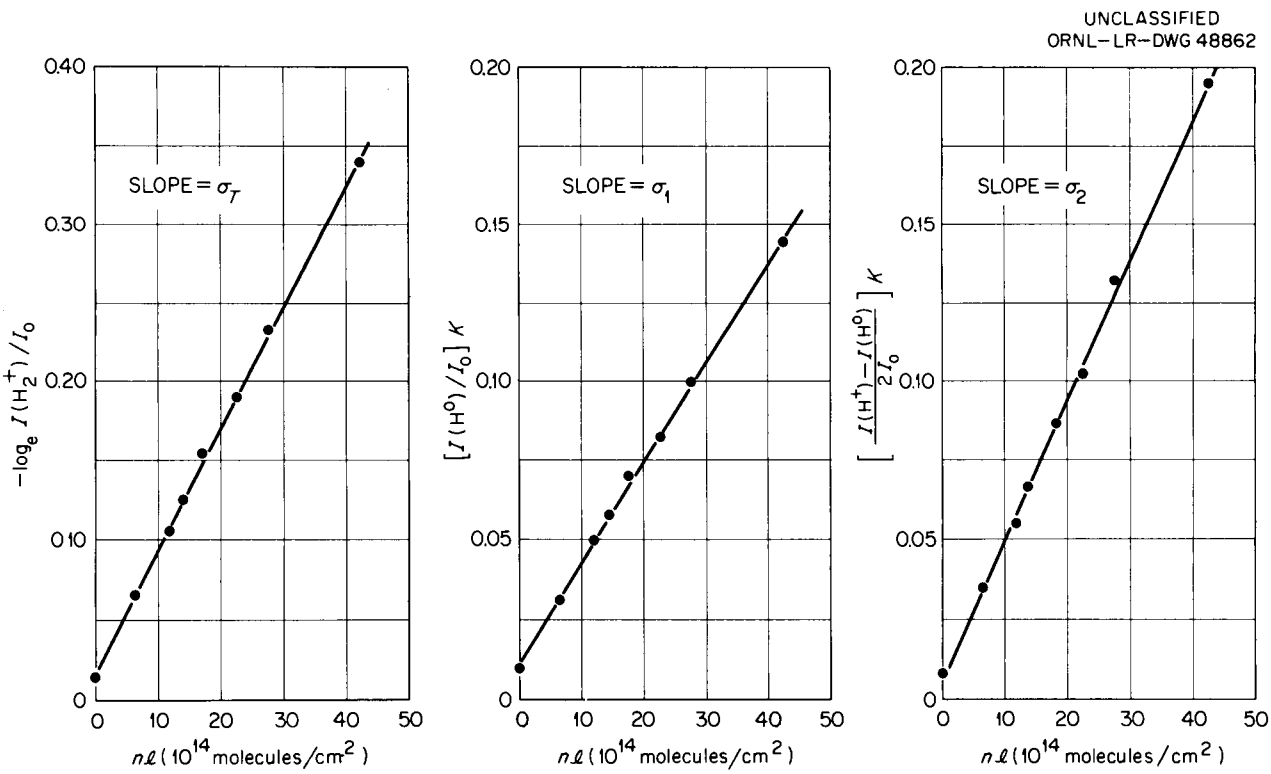

Fig. 2. Variation of Beam Current Ratios with Pressure Changes for 600-kev H_2^+.

$$\sigma_2 nl + C = \frac{I(H^+) - I(H^0)}{2I_0} \left\{ -\frac{\log_e [I(H_2{}^+)/I_0]}{1 - [I(H_2{}^+)/I_0]} \right\}$$

$$= \frac{I(H^+) - I(H^0)}{2I_0} K \ . \qquad (3')$$

The values A, B, and C also result from the measurement of the currents when $n = 0$. This was confirmed experimentally by shutting off the gas supply and measuring the currents, giving A, B, and C directly.

It is assumed implicitly in this method that the relative background-gas composition as well as total background is constant; that is, the background does not change as more hydrogen is admitted into the gas cell to raise the pressure. However, there is evidence (*4*) from other experiments that in admitting hydrogen gas into a system, the background gases can also increase in pressure – at least in going from 10^{-7} to 10^{-5} mm Hg for H_2. The change in background is believed to be unimportant in the pressure range used in this experiment (10^{-4} to 10^{-3} mm Hg).

In the region where cross sections σ_3 and σ_4 become important (below 300 kev), the measured cross sections σ_1 and σ_2 must be corrected to get the "true" cross sections σ_1 and σ_2. Calling $\sigma_0 = \sigma_3 + \sigma_4$, then from the method of measuring currents that was used, the corrected (primed) cross sections are related to the measured ones (unprimed):

$$\sigma_1' = \sigma_1 - 2\sigma_0 \ ,$$

$$\sigma_2' = \sigma_2 + \sigma_0 \ ,$$

$$\sigma_T' \equiv \sigma_1' + \sigma'_2 + \sigma_0 = \sigma_T \ ,$$

$$\sigma_p' = \sigma_p \ .$$

The values used for σ_0 may be taken from Sweetman's (*3*) results for $H_2{}^+$ at energy E or from Barnett's results (*2*) for $H^+ \rightarrow H^0$ at energy $E/2$. It should be noted that σ_T and σ_p do not depend on these corrections.

At high pressures (in practice for P greater than 3×10^{-3} mm Hg), the slopes of the lines resulting from plotting Eqs. (2′) and (3′), σ_1 and σ_2, may depart from linearity because of multiple collisions – the dissociation collision being followed by a charge-exchange collision (e.g., $H_2{}^+ \rightarrow H^0 + H^+ \rightarrow 2H^+$; $H_2{}^+ \rightarrow 2H^+ \rightarrow 2H^0$). Thus, the cross sections σ_1 and σ_2 were taken only from that range of nl over which the slope was linear.

Independent runs that were made in order to check the reproducibility of the results agreed to 3% with the previous runs at the same energy.

RESULTS

Cross Sections

The primary purpose of this experiment was to resolve the discrepancies among the published data on the dissociation of $H_2{}^+$ by H_2; however, even though agreement with a set of published data is encouraging as a step toward resolving differences, it does not provide a firm basis for discounting the other data. Nonetheless, confidence in one's own results and internal consistency of the data, coupled with agreement with another carefully done experiment, provide a bias for that agreement. The results of this experiment (displayed together with published data in Figs. 3 and 4) show good agreement with Sweetman up to 500 kev, but agree more closely with Barnett for the higher energy. The investigators have been: Sweetman (*3*) (100 to 800 kev); Barnett (*5*) (20 to 200 kev; 500 to 2250 kev); Fedorenko (*6*) (5 to 180 kev); Damodaran (*7*) (100 to 220 kev); and Postma and Hamblen (200 to 600 kev).

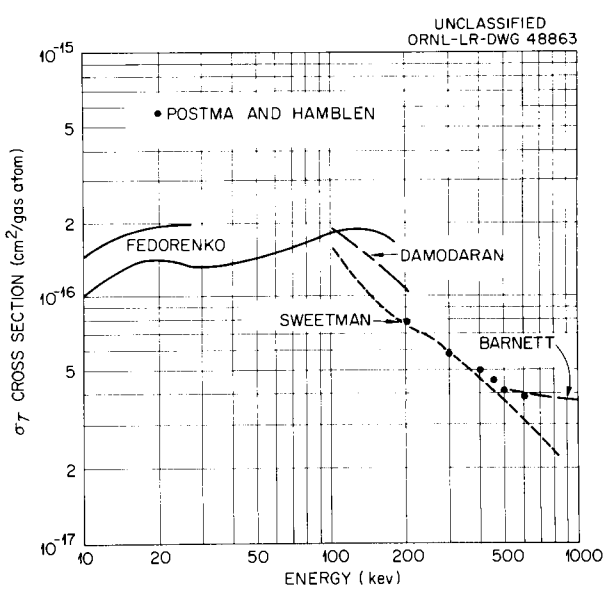

Fig. 3. Total Cross Section for $H_2{}^+$ Loss in H_2.

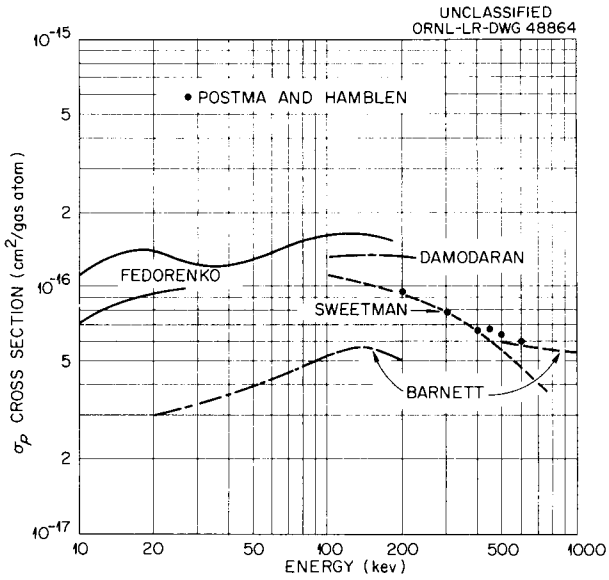

Fig. 4. Proton-Production Cross Section for H_2^+ in H_2.

Because of a lack of detailed information in the published papers, it is difficult to judge them and to find points that may lead to erroneous results. Thus, one can only plot the data and hope that experiments done in widely different ways might group together and present a concerted front of agreement.

The low-energy (20 to 200 kev) results of Barnett (5) are not in accord with the other experiments, which, although not agreeing among themselves too well, at least are grouped closely. Since all the details of Barnett's experiment are not known, it is not possible to show where any discrepancy might be.

Neither is it possible to tell from Fedorenko's experiments how the calculations were carried out and how the corrections were applied. Damodaran performed the dissociation measurements in much the same fashion as done in the present experiment, but he didn't consider the production of H_2^0 or $2H^0$, and not enough details are given in his publication to know whether his calculations are independent of a knowledge of these.

The results of Sweetman are detailed; the internal consistency of the data is presented together with the extent of all corrections. His ability to measure all four partial cross sections (σ_1, σ_2, σ_3, and σ_4) gives the most complete picture of the processes going on in the dissociative reaction.

Although the agreement between Sweetman's experiment and this experiment may be fortuitous, the different methods of measurement of the reactions, the checks incorporated into the measurements, and the methods of calculation all support the contention that the grouping of these separate measurements is probably a genuine agreement.

The errors of this experiment were mainly confined to pressure uncertainties (4%), beam fluctuations (7%), correction uncertainties (10%), and energy uncertainties (3%), and all combine to place limits of confidence close to ±15%.

The departure of agreement with Sweetman's data at high energies still is without explanation, even though it is only slightly outside experimental error. The trend of the present data certainly shows agreement with Barnett's high-energy results, but it is most evident from the present work that Barnett's low-energy results do not fall in the region of the other data.

Angular Distributions

An energetic H_2^+ in collision with a target molecule may be excited into a repulsive state by making an electronic transition which obeys the Franck-Condon principle. Classically, the individual particles resulting from such a dissociative transition share the energy equally and are isotropically distributed in space in the center-of-mass system. The dissociated H^0 and H^+ from a beam of H_2^+ thus acquire a slight angular deviation from the original direction of the H_2^+ beam. A simple classical picture in which the H_2^+ breaks up to release two particles of equal mass (sharing equally the energy of dissociation) results in a calculated rms angular spread about the original beam direction of

$$\overline{\Delta\theta^2} = \frac{\overline{\Delta E}}{2E} , \qquad (4)$$

where

$\overline{\Delta\theta^2}$ = the rms angle between the dissociated particle and the beam direction,

$\overline{\Delta E}$ = the energy acquired by the dissociated particle in the breaking-up process, and

E = the energy of the incident H_2^+ particle.

Figure 5 shows the electronic states of H_2^+ (ref 8). An electron transition to the $H^0 + H^+$ repulsive state ($^2\Sigma_u$) gives the pair of particles approximately 8 ev of energy while a transition to the $H^+ + H^+$ repulsive state gives that pair

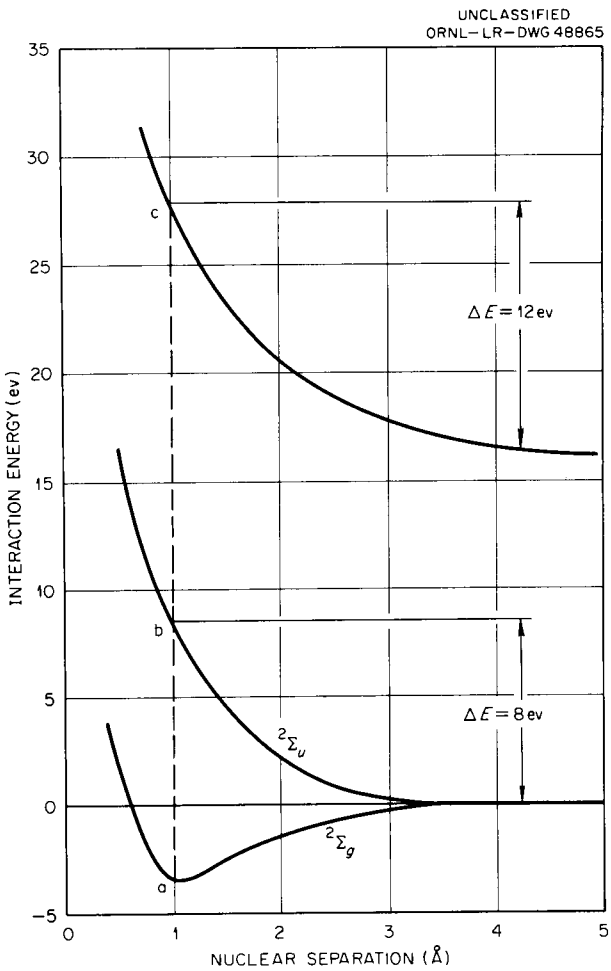

Fig. 5. Potential Energy Curves for Electronic States of H_2^+.

approximately 12 ev of energy. From the average energy per particle (4 and 6 ev, respectively) and the initial energy of H_2^+, the rms angle may be found. In fact, from the experimental determination of the $\overline{\Delta\theta^2}$ it should be possible to find the average energy $\overline{\Delta E}$. However, with a long target cell such as the one used in this work, all the reactions do not occur at a single point but are equally probable along the entire path of the beam in the gas cell. While the *angular* spread is the same everywhere, the *linear* spread at the exit aperture depends upon where the reaction took place in the cell. Thus, the linear width of the distribution of current coming out of the cell is proportional to the rms angle, and the square of the width should obey the $1/E$ dependence of Eq. (4) also.

Since all the beams were scanned, it was possible to observe the widths of these beams at the exit aperture. Figure 6 shows typical widths of H_2^+ and H^+ beams for incident 200-kev H_2^+. By convolution of the two curves, the effect of the spread of the incident H_2^+ beam may be subtracted to leave only the spread of the H^+ (or H^0) resulting from the dissociation process. If a characteristic of this H^+ beam spread (full width at half height, which is proportional to $\overline{\Delta\theta^2}$) is multiplied by E, then the result, $K\overline{\Delta\theta^2}E$, should be constant with energy changes if Eq. (4) describes the dissociation. This resulting constant is then proportional to $\overline{\Delta E}$. Figure 7 shows the result of plotting the product $K\overline{\Delta\theta^2}E$ vs E. The line drawn through the experimental points is a best guess, and there was no attempt to find $\overline{\Delta E}$ from this data.

This points out strongly that one must be very careful to have large enough exit apertures to ensure collection of all the broken-up beams. The data shows that if the entrance and exit aperture were of the same diameter, then σ_p would be too low by more than a factor of 2 at 200

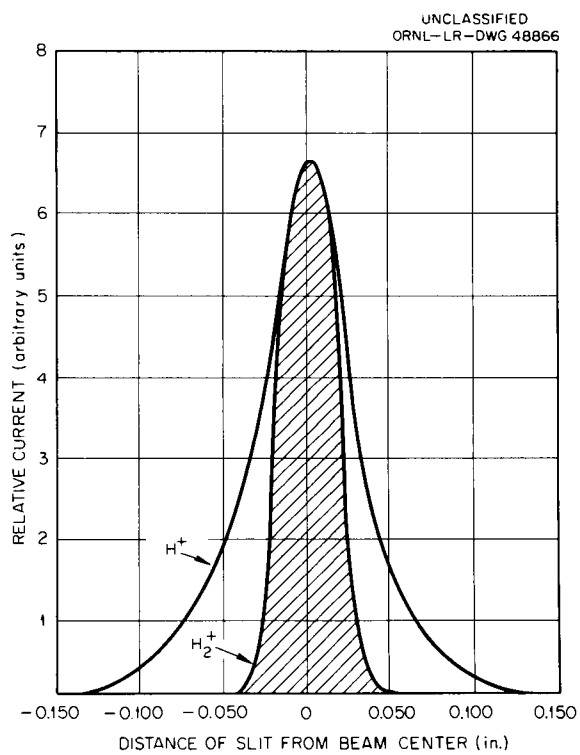

Fig. 6. Beam Widths at 200 kev.

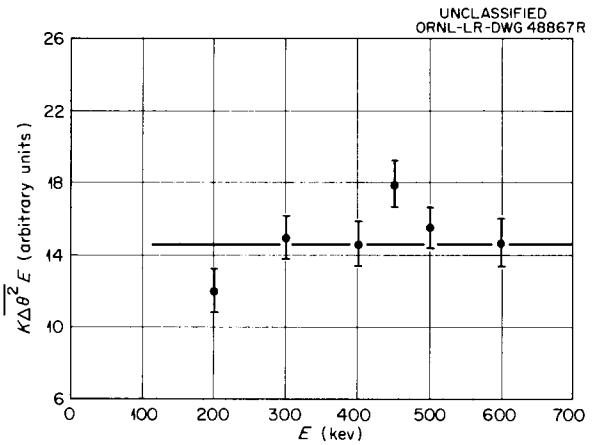

Fig. 7. Angular Spread of Dissociated H_2^+ Products as a Function of Energy of H_2^+.

kev. Experimentally, this reduction in cross section was measured at 300, 400, and 500 kev, with an entrance aperture of $\frac{1}{16}$ in. diameter, and an exit aperture of $\frac{3}{32}$ in. diameter. The reduction for σ_p was 1.75 at 300 kev, 1.50 at 400, and 1.27 at 500. The linear spread depends strongly on the gas-cell length. This is perhaps a reason for Barnett's cross sections being lower at the low energies than the other reported measurements.

Attempts to calculate theoretically the dissociation cross section by using the Born approximation have been made by Salpeter (*9*) and by Gerjuoy (*10*). The extension of their predictions into the lower energy region where our work was done is not adequate in accounting for the dissociation cross section.

Plans are under way to extend these measurements to other target gases and also to lower energies by using detection techniques which yield better energy resolution.

REFERENCES CITED

(*1*) R. Fraser, *Molecular Beams*, Methuen, London, 1937.

(*2*) C. F. Barnett and H. K. Reynolds, "Charge Exchange Cross Sections of Hydrogen Particles in Gases at High Energies," *Phys. Rev.* **109**, 355 (1958).

(*3*) D. R. Sweetman, "Dissociation of H_2^+ Ions by Hydrogen," *Phys. Rev. Letters* **3**, 425 (1959).

(*4*) G. R. Haste, ORNL Thermonuclear Experimental Division, private communication.

(*5*) C. F. Barnett, "The Dissociation of Diatomic Hydrogen Ions," *Proc. U.N. Intern. Conf. Peaceful Uses Atomic Energy, 2nd, Geneva, 1958* **32**, 398 (1959).

(*6*) N. V. Fedorenko *et al.*, "Dissociation of the Molecular Ion H_2^+ in Collisions with Gases," *Zhur. Tech. Fiz.* **24**, 769 (1954); *Soviet Phys. JETP* **36**(9), 267 (1959).

(*7*) K. K. Damodaran, "Dissociation of Molecular Hydrogen Ions (H_2^+) in Gases," *Proc. Roy. Soc. (London)* **239A**, 382 (1957).

(*8*) H. S. W. Massey and E. H. S. Burhop, *Electronic and Ionic Impact Phenomena*, Oxford, 1952.

(*9*) E. E. Salpeter, "Dissociation Cross Sections for Fast Hydrogen Molecule Ions," *Proc. Roy. Soc. (London)* **63A**, 1295 (1950).

(*10*) E. Gerjuoy, *Dissociation and Ionization of H_2^+ by Fast Protons*, Research Report 60-94439-1-R2, Westinghouse Research Laboratories, Pittsburgh, Penna. (1955).

INTERNAL DISTRIBUTION

1. C. E. Center
2. Biology Library
3. Health Physics Library
4–5. Central Research Library
6. Reactor Experimental Engineering Library
7–26. Laboratory Records Department
27. Laboratory Records, ORNL R.C.
28. A. M. Weinberg
29. L. B. Emlet (K-25)
30. J. P. Murray (Y-12)
31. J. A. Swartout
32. E. H. Taylor
33. E. D. Shipley
34. A. H. Snell
35. M. L. Nelson
36. W. H. Jordan
37. G. E. Boyd
38. R. A. Charpie
39. S. C. Lind
40. F. L. Culler
41. A. Hollaender
42. J. H. Frye, Jr.
43. M. T. Kelley
44. J. L. Fowler
45. R. S. Livingston
46. K. Z. Morgan
47. T. A. Lincoln
48. A. S. Householder
49. C. P. Keim
50. C. E. Winters
51. D. S. Billington
52. E. P. Blizard
53. M. J. Skinner
54. P. Lafyatis
55. D. P. Hamblen
56–64. H. Postma
65. C. Parker
66. A. Simon
67. M. Rankin
68. D. T. Goldman
69. E. Ivash
70. P. R. Bell
71. J. S. Luce
72. C. F. Barnett
73. C. D. Moak
74. R. J. Mackin, Jr.
75. W. F. Gauster
76. O. C. Yonts
77. W. R. Chambers
78. R. V. Neidigh
79. H. C. Hoy
80. J. R. McNally
81. T. K. Fowler
82. E. Guth
83. R. A. Dandl
84. P. M. Reyling
85. R. S. Cockreham
86. W. G. Stone
87. J. Neufeld
88. W. D. Manly
89. R. E. Clausing
90. T. A. Welton
91. C. E. Normand
92. G. F. Leichsenring
93. R. L. Knight
94. C. W. Blue
95. C. H. Weaver
96. R. J. Kerr
97–98. Sherwood Reading File (1 copy ea. to V. Glidwell and P. R. Bell)
99. W. P. Allis (consultant)
100. D. W. Kerst (consultant)
101. L. P. Smith (consultant)
102. ORNL – Y-12 Technical Library, Document Reference Section

EXTERNAL DISTRIBUTION

103. Division of Research and Development, AEC, ORO
104–713. Given distribution as shown in TID-4500 (15th ed.) under Physics and Mathematics category (75 copies – OTS)